EXPERIMENTAL TECHNIQUE TO CHARACTERIZE MACROBENDING LOSS IN SINGLE MODE FIBER

By: Girum Getu

A thesis submitted to the school of graduate studies of Addis Ababa University in partial fulfillment of the requirements for the degree of Masters of Science in Materials Science

June 2010

ADDIS ABABA UNIVERSITY

GRADUATE STUDIES

Experimental Technique to characterize Macrobending Loss in Single Mode Fiber

By: Girum Getu

Materials Science Program
Faculty of Science

Approved by the Examining Board

Prof.A.V.Gholap ______________________________
(Advisor)

Dr.Araya Asfaw ______________________________
(Examiner)

Dr.S.K.Ghoshal ______________________________
(Examiner)

Prof.Teketel Yohannes ______________________________
(Chairperson)

Acknowledgements

Firstly, I would like to thank the ALMIGHTY GOD with his MOM for giving me health, the patience and the effort for all the unforgettable rough times, and come to an accomplishment of this paper.

Then after, I would like to express my gratitude to the following people for their involvement and/or support with this thesis work:

I would like to express my utmost gratitude to Prof. Ashok V. Gholap, my thesis Supervisor, for providing me with an opportunity to work on this thesis and sharing his fiber optic expertise. His commitment, constructive criticism, treatment and guidance have been invaluable to the completion of this paper and interest in thesis advice was greatly appreciated during a year stay with him.

I would like to acknowledge Prof.Teketel Yohannes, Director of the Materials Science Program, for his encouragement, treatment, concern, friendly but serious approach and close follow up for this to happen.

I would like to acknowledge Mr.Tesfaye Mamo of the advanced optic lab assistant of Addis Ababa University who helped me with spending some sleepness night and Ministry of science and Technology for their great help and superb enthusiasm in the support of Lab equipments, especially Eng. Abebayehu Mamo and the technical assistant Mesfin Gebeyehu.

I would also like to express my deepest heartily feeling and grateful thanks for my family, my father Getu Adera, my mother ATSEDE MEKURIA, my sisters: Jerusalem Getu particularly for my elder sister Genet Getu, who has got a special place in my whole life, and my brothers Melesew Tefera, and Mengesha Belay for their moral and financial assistant in my academic achievement.

Last but not least special thanks go to: Mulualem Abebe, Henok Tsegaye, Abeje Aychiluhem, Dereje Mekonnen, Haftom Reda, Mintayhu Hussen and Messay Betru.

Table of Contents

Acknowledgement iii

List of Tables vi

List of Figures vii

List of Appendices viii

Acronyms ix

Abstract x

1. Introduction …………………………………………………………….1

1.1 Objective and Motivation …………………………………………………..2

1.2 Structure of the thesis…………………………………………………………..4

2. Over View Step-index Fiber optic in Signal Degradation …………...5

2.1 Introduction ……………………………………………………………………...5

2.2 Optical confinement ……………………………………………………………..5

2.3 Fundamentals of light …………………………………………………………...7

2.3.1 Electromagnetic Spectrum ………………………………………………..7

2.4 Signal propagation in optical fiber …………………………………………….8

2.4.1 Light propagation in an optical fiber ……………………………………..8

2.4.2 Propagation of Fiber Modes ……………………………………………….9

2.4.3.1 Step-index Single Mode Fibers ……………………………………..9

2.4.3.2 Mode coupling ……………………………………………………….10

2.4.3.3 Cladding Modes and Leaky Modes ………………………………..11

2.4.3.4 Power density distribution …………………………………………...12

2.4.3.5 Evanescent wave ……………………………………………………..13

2.4.3.6 Gaussian Approximation ……………………………………………..14

2.4.3.7 Spot Sizes …………………………………………………………….15

2.4.3.8 Gaussian Beams ……………………………………………………...15

2.5 Fiber losses ………………………………………………………………..16
2.5.1 Attenuation …………………………………………………………….17
2.5.2 Scattering …………………………………………………………...18
2.5.3 Absorption Losses ……………………………………………………..21
2.5.4 Radiation Losses ……………………………………………………24
2.5.4.1 Bending Loss in Optical Fiber …………………………………..24

3. Method and Materials ………………………………………………..30
3.1 Materials …………………………………………………………………….30
3.2 Methods...…………………………………………………………………..30
3.2.1 Measurement using He-Ne laser without macrobending ……………………..31
3.2.2 Measurement using Mercury Vapor Lamp without macrobending …………..32
3.2.3 Measurement for macrobending loss…………………………………….....32
3.2.4 Theoretical Calculation of Fiber bend loss……………………………………33

4. Result and Discussion….. ………………………………………………..35
4.1 Measurement without macrobending …………………………………………...35
4.2 Measurement with macrobending ………………………………………….....36
4.3 Data error Analysis ………………………………………………………......41

5. Conclusion …………………………………………………………43

6. Reference …………………………………………………………...44

Appendices ………………………………………………………….46

List of Tables

Table 4.1 Loss without Macrobending …………………………………………………..35

Table 4.2 Bend Loss due to bending for different wavelength………………………. …37

Table 4.3 Bend Loss due to bend radius of curvature for λ= 633nm ……………………38

Table 4.4 Bend Loss due to bend radius of curvature for λ= 546nm …………………...40

Table 4.5 The dependence of C_R and C_α with the variation of the different wavelengths ……………………………………………………..41

List of Figures

Figure 2.1: Planar interface geometry …………………………………………………… 6
Figure 2.2: Electromagnetic Spectrum ………………………………………………….. 7
Figure 2.3: Removal of cladding power by a mode stripper …………………………… 12
Figure 2.4: Typical spectral attenuation in silica ………………………………………. 17
Figure 2.5: Scattering and Absorption losses …………………………………………... 20
Figure 2.6: Schematic showing the geometry of a fiber bend …………………………. 25
Figure 2.7: Schematic showing shift of the peak of the field away from the center of Curvature of the fiber …………………………………………………….. 26
Figure 2.8: An extra loss due to macrobending on the basic fiber loss …………………28
Figure 2.9: Power lost and field distribution in a bend fiber …………………………... 28
Figure 3.1: Experimental set up for He-Ne laser ………………………………………. 31
Figure 3.2: Experimental set up for He-Ne laser with macrobending………………….. 32
Figure 3.3: Experimental set up for Mercury Vapor lamp ………………………………33
Figure 4.1: Attenuation Coefficient Vs Bend Radius of Curvature ……………………..37
Figure 4.2: Bend loss vs. Bend Radius of Curvature for λ=633nm ……………………. 39
Figure 4.3: Bend loss vs. Bend Radius of Curvature for λ=546nm ……………………. 40

List of Appendices

Appendix A …………………………………… ………………………………….. 46

Appendix B…………………………………………………………………………48

Acronyms

a.u	Arbitrary Unit
FTTH	**F**iber-**t**o-**t**he-**H**ome
IR	**I**nfra**r**ed
ITU-T	**I**nternational **T**elecommunication **U**nion-**T**esting
LASER	**L**ight **A**mplification **S**timulated by **E**lectromagnetic **R**adiation
MDUs	**M**ultiple-**D**welling **U**nits
MFD	**M**ode **F**ield **D**iameter
NA	**N**umerical **A**perture
ppm	**p**arts **p**er **m**illion
SMF	**S**ingle **M**ode **F**iber
SFUs	**S**ingle-**F**amily **U**nits
UV	**U**ltra **V**iolet

Abstract

An experimental technique of macrobending losses for a single mode fiber (SMF) with different radius of curvature is presented. Macrobending losses for SMF are investigated experimentally, showing that a tight bent of fiber has a significant impact on the power loss. This experimental measurement suggests how this method is crucial to characterize macrobending at wavelength of interest even to calculate the power loss due to bending, to determine the spectral window at which the fiber can effectively operates, to predict the bend loss for a higher wavelength from the trend of shorter wavelengths. This thesis work also investigates the variation of the constants, C_R and C_α , which depends on the waveguide dimension, with respect to shorter wavelengths using He-Ne laser and Mercury Vapor Lamp sources of light that emits different wavelengths in the visible and ultraviolet region of an optical spectrum using an optic beam launch method.

Corresponding experimental tests are presented, which agree with the theoretical results that show, the bent fiber at different bend radii has a significant influence on the total loss of the fiber.

Key words: macrobending ; optic beam launch; optical spectrum; radius of curvature: Single mode fiber: spectral window; power loss

Declaration

I, the undersigned, declare that this thesis work is my original work, has not been presented for a degree in this or any other universities, and all sources of materials used for the thesis work have been fully acknowledged.

Name: Girum Getu Signature: ______________________

Place: Addis Ababa

Date of submission:

This thesis has been submitted for examination with my approval as a university advisor.

Prof.A.V.Gholap Signature: ______________________

Advisor's Name

Yours sincerely,

1. Introduction

1.1 Introduction

An optical fiber is a dielectric waveguide made of glass or plastic consisting of a core, cladding and a sheath or jacket. The index of refraction of the assembly varies across the radius of the cable, with the core having a constant or smoothly varying index of refraction and the cladding region having another constant index of refraction. The core possesses a high refractive index, where as the cladding is constructed to have a lower refractive index. The result of the difference in the refractive indexes is to keep light flowing through the core after it gets in to the core, even if the fiber is bent or tied in to a knot, through total internal reflection.

The choice of fiber optic cables in telecommunications lies on its advantage over copper such as, very high bandwidth, resistance to electromagnetic noise, large carrying capacity, longer transmission high speed and costs much less to maintain. Recently, because of their cost effectiveness and better quality, fibers have been used to replace copper wire as an appropriate means of communication and signal transmission. Even if, optical fibers have these advantages, signal attenuation and distortion are important degradation factors in limiting the transmission systems. [1]

Attenuation is the loss of optical power as light travels along the fiber. It is a result of absorption, scattering, bending, and other loss mechanisms. Each loss mechanism contributes to the total amount of fiber attenuation. Of importance to this study is power loss due to bending specifically macrobending. Macrobends are bends having a large radius of curvature relative to the fiber diameter. These bends become a great source of loss when the radius of curvature is less than several centimeters. [2]

Any dielectric waveguide will radiate if it is not absolutely straight. The bending of a dielectric waveguide produces a source of radiation loss in the cladding even if the propagating ray is greater than the critical angle.

To maintain a guided mode field with equiphase fronts on radial planes, a fraction of the mode field on the outside of the bend would have to exceed the plane wave velocity in the cladding medium. Since this is impossible, the energy associated with this part of the mode field is lost to radiation. The radiation attenuation coefficient α_{bend}, with radius of curvature R, has the form

$$\alpha_{bend} = C_{\alpha} \exp(-C_R R) \qquad (1.1)$$

Where C_R and C_{α} are constants that will characterize the attenuation coefficient. [3]

1.2 Motivation and Objective

Light power propagating in a fiber decays exponentially with length due to absorption and scattering losses. Attenuation is the single most important factor determining the cost of fiber optic telecommunication systems as it determines spacing of repeaters needed to maintain acceptable signal levels. In the near infrared and visible regions, the small absorption losses of pure silica are due to tails of absorption bands in the far infrared and ultraviolet. Impurities-notably water in the form of hydroxyl ions-are much more dominant causes of absorption in commercial fibers. Recent improvements in fiber purity have reduced attenuation losses. State-of-the-art systems can have attenuation on the order of 0.1dB/km. Scattering can couple energy from guided to radiation modes, causing loss of energy from the fiber. There are unavoidable Rayleigh scattering losses from small scale index fluctuations frozen in to the fiber when it solidifies. This produces attenuation proportional to Rayleigh scattering, $1/\lambda^4$.

The optical fibers for telecommunications are required to operate with the lowest attenuation loss at a wavelength of about 1550nm. As the requirement for optical performance of optical fibers is stringent, the source of attenuation loss in optical fiber needs to be eliminated at a wavelength of about 1550nm. However, certain physical constraints in which the optical fibers can be used result in increase in attenuation loss of the fiber and an important one of these physical constraints is bending loss of the fiber, which is introduced during bending of the fiber while transporting and installation. Therefore, if bending loss of a fiber increases it results in increase in the attenuation loss of the fiber.

In an optical fiber produced by conventional method, the signal losses of substantial level may be introduced either by turning the fiber about a point with relatively smaller radius of curvature or by waviness introduced during the sheathing of the fiber. It has been observed that a planar wave front, which must propagate through a bend, has different path lengths between the center of the core and its outer radius. A shift in mode field diameter of fiber on its bending has been observed to result in energy losses thereby resulting in increase in bending loss of the fiber. These losses are known as macrobending losses and have been found to be dependent up on the extent of the bending that is introduced in the fiber. If radius of curvature of the bend of the optical fiber is smaller and wavelength of transmitted light is longer, the macrobending loss in optical fiber has been observed to increase. Furthermore, the macrobending loss caused by loss of power due to radiation at optical. It has been observed that below a critical radius optical fiber bending, the macrobending loss in optical fiber becomes significant and noticeable. There is also a need to have optical fiber having reduced macrobending loss and attenuation loss, thereby being suitable for access communication network applications.

Furthermore, the ever-increasing demand for bandwidth in the residential sector and long haul transmission has pushed fiber optics manufacturers, service providers and researchers to develop Fiber-to-the Home technology (FTTH) and long line transmission. Fiber transmission capacity, 25Tbp, of all the mediums, but it is not as rugged and forgiving as copper. Current fiber in homes, buildings and long haul transmission experience in loss signal strength because fiber has to routed round tight corners and many turns in the long line respectively, making it complicated and expensive to install. Mostly holes has to be drilled through walls for FTTH, high way roads will be dug and even sometimes buildings will be destructed for long haul in order to avoid bending the fiber optic cable making it fiber installations visually unappealing. Service providers like Verizon and fiber optic manufacturers like Corning and researchers are working closely together to develop fiber that can handle the smaller bend radii encountered in Single-family units (SFUs), Multiple-dwelling units(MDUs), in-home wiring and long line wiring. [4]

In view of all these, it is indispensable:

- to calculate power loss due to macrobending
- to predict bend loss of the fiber and the spectral window at which a fiber can operate effectively

-to obtain the relationship between constant C_R and C_α against the wavelength and the variation of these constants with the wavelength

-and also to predict the intrinsic loss of the fiber and the dominant nature of scattering in short wavelengths, particularly in the visible region

1.3 Structure of the thesis

Chapter 1 gives an introduction of the power loss due to macrobending and the objective of the thesis

Chapter 2 gives an extensive coverage of the theoretical background of attenuation associated with macrobending in particular and losses that are related to macrobending during signal propagation in an optical fiber in general. In addition, parameters that affect macrobending will be discussed.

Chapter 3 is all about experimental technique to measure bending loss for shorter wavelengths using He-Ne laser and Mercury Vapor Lamp

Chapter 4 provides the outcome of the measurements performed with and without bending of the fiber

Chapter 5 concludes the thesis and highlight recommendation for future work

2. OVERVIEW OF FIBER OPTICS IN SIGNAL DEGRADATION

2.1 Introduction

This chapter deals with the basics of optical fiber propagation and some of the fiber parameters that are used to characterize signal degradation. It begins by describing the confinement process that makes optical fibers useful, defining several parameters, and introducing several terms that are associated with optical fiber. Moreover, it briefs out propagation of various electromagnetic modes and the signal degradation while the mode propagates in an optical fiber. [5]

2.2 Optical confinement

Optical fibers work by confining the light within a long strand of glass. In their simplest form, they are cylindrical dielectric waveguides made of central cylinder of glass with one index of refraction, surrounded by an annulus with slightly different index of refraction.

One confinement process that traps the light inside the fiber and allows it to propagate down the length of the fiber based on the principle of total internal reflection at the interface of the two dielectric media. Consider an optical-plane-wave incident on an infinite planar interface between two dielectric media, as shown in Fig.2.1. The propagation direction of the plane wave makes an angle of incidence θ_i with the normal to the interface as shown in the figure. The index of refraction (or refractive index) n of a medium is given by the equation

$$n = \frac{c}{V} \tag{2.1}$$

where c is the velocity of light in a vacuum ($3x10^8$m/sec) and v is the velocity of light in the medium. (Note that n is always greater than 1; for glass, n is between 1.4 and 1.5) For total internal reflection to occur, the index of refraction of the medium containing the incident plane wave is required to be larger than the index of refraction of the other medium (i.e., the wave is traveling from the higher-index medium in to the lower- index medium).

Snell's law governs the transmission of the plane wave through the interface and is given by

$$n_1 \sin\theta_i = n_2 \sin\theta_t \qquad (2.2)$$

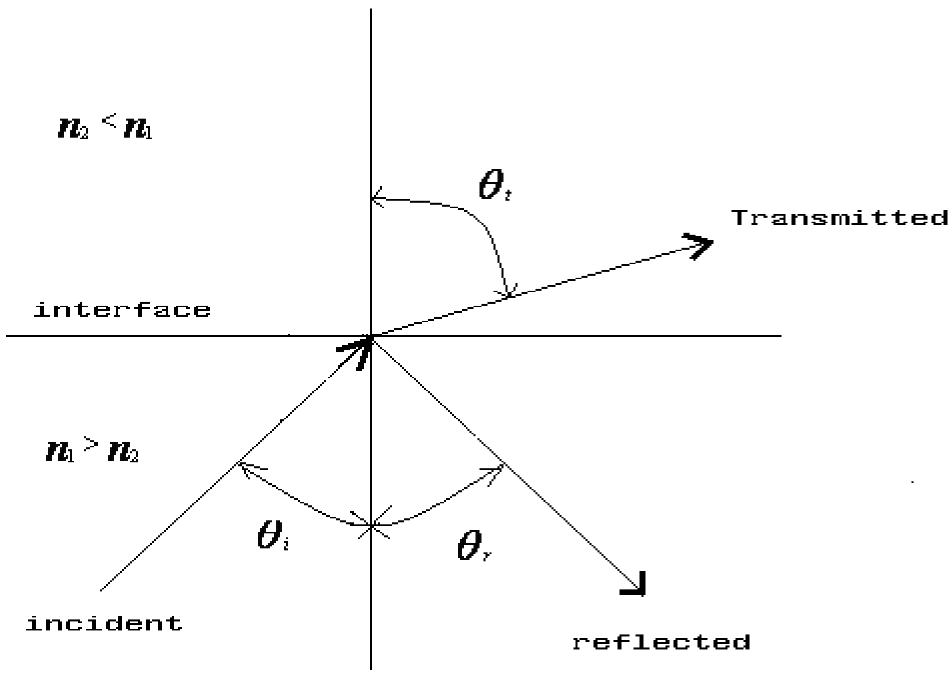

Figure 2.1: Planar interface geometry.

where θ_i is the angle of incidence and θ_t is the angle of transmission. From this relation, one can see that θ_t reaches 90 degrees when θ_i reaches the value of

$$\theta_i = \theta_c = \sin^{-1}\left(\frac{n_2}{n_1}\right) \qquad (2.3)$$

where is called the critical angle of incidence and is given by the latter part of the equation. For angles of incidence equal to or exceeding the critical angle, the energy of the incident wave is totally reflected back in to medium. It is this total internal reflection that allows the light to propagate with no loss. Light that is incident at an angle below the critical angle is partially transmitted and partially reflected, losing a significant fraction of the power in to the transmitted beam.

2.3 Fundamentals of light

In this section of the thesis those fundamental characteristics and phenomenon of light that relate to fiber optics will be discussed. The discussion to those principles of light that is relevant to a basic understanding of optical fibers. [6-9]

2.3.1 Electromagnetic Spectrum

Fundamentally, there is no difference between light waves and other electromagnetic waves, such as radio and radar, except that light waves are much shorter and therefore have a much higher frequency. When all types of electromagnetic radiation are arranged in order of wavelength, the result is called the electromagnetic spectrum, shown in

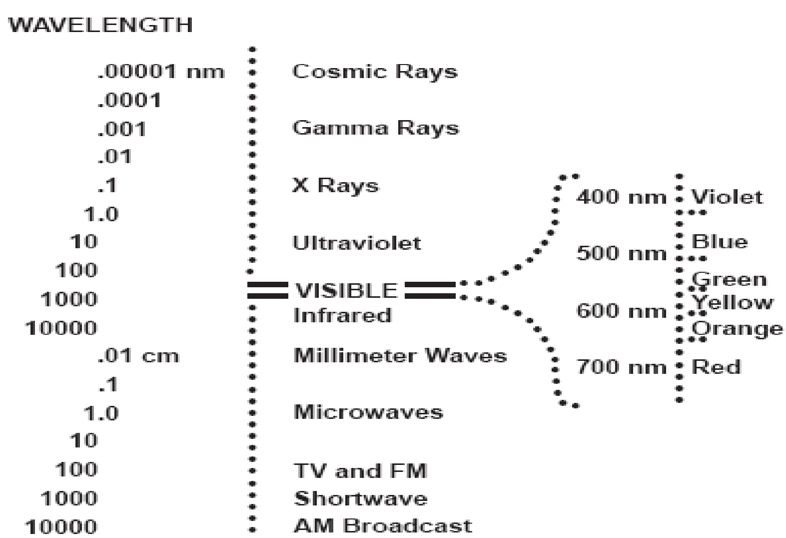

Figure 2.2: Electromagnetic Spectrum

Notice how broad this range is: from long electrical oscillations with wavelengths measuring thousands of kilometers to cosmic rays with wavelengths in trillionths of a meter. There are no gaps in the spectrum, but some of the regions overlap or blend. That is, the boundary between regions is not sharp.

As can be seen in Fig.2.2, optical radiation lies between microwaves and x-rays. It includes all wavelengths between 10nm and 1mm. Within this range, as shown on the left side of fig.2.2, are ultraviolet, visible light, and infrared radiation. The term visible light seems redundant; however, it is necessary because ultraviolet and infrared light, respectively. Visible light is defined as that radiation which stimulates the sense of sight. It includes all radiation from 390nm to 770nm, from violet to red. Obviously, the visible spectrum is just a small fraction of the electromagnetic spectrum.

In fiber optics, a typical wavelength is 820nm. From fig.2.2 it is clearly seen that this radiation is designated infrared, although it is sometimes referred to as light because it can be controlled and measured with instruments similar to those used for visible light. [10]

2.4 Signal propagation in optical fiber

Optical fiber is a remarkable communication medium compared to other media such as copper or free space. An optical fiber provides low-loss transmission over an enormous frequency range of at least 25THz-even higher with special fibers which are orders of magnitude more than the bandwidth available in copper cables or any other transmission medium. For example, this bandwidth is sufficient to transmit hundreds of millions of phone calls simultaneously, or tens of millions of Web Pages per second. The low-loss property allows signals to be transmitted over long distances at high speeds before they need to amplified or regenerated. It is due to these two properties of low loss and high bandwidth that optical fiber communication systems are so widely used today.

2.4.1 Light propagation in an optical fiber

Signal propagation in optical fibers can be described by either geometrical optics or Maxwell’s equations. Geometrical optics is a good approximation when the wavelength of light is very small compared to the system’s dimensions. On the other hand, Maxwell equations can tell the exact story but is much more mathematically complex.

This section uses both methods to study light propagation, but avoids complex mathematics such as solving wave equations in optical fiber. Instead, it stresses the relationship between geometrical optics and wave function. This approach shows the insight of the physics of light wave propagation with minimal mathematics.

2.4.3 Propagation of Fiber Modes

The electric and magnetic field vectors in the core, $\tilde{E}_{\text{core}}$ and $\tilde{H}_{\text{core}}$, and the electric and magnetic field vectors in the cladding, $\tilde{E}_{\text{cladding}}$ and $\tilde{H}_{\text{cladding}}$, must satisfy the wave equations, 2.10 and 2.11, respectively. However, the solution in the core and the cladding are not independent; they are related by boundary conditions on E and H at the core-cladding interface. Quite simply, every pair of solutions of these wave equations that satisfies these boundary conditions is a fiber mode. Only a finite set of wave functions satisfying the Maxwell equations can propagate in a fiber, each of which is called a propagation mode.[11]

2.4.3.1 Step-index Single Mode Fibers

When a light wave propagates inside the core of a fiber, it can have different electromagnetic field distributions over the fiber cross-section. Each field distribution that meets the Maxwell equations and the boundary condition at the core-cladding interface is called a transversed mode. Fibers that allow propagation of only one transverse mode are called single mode fibers (SMF) but fibers that support more than one transverse mode are Multimode fibers.

2.4.3.1.1 Cutoff Wavelength

For small values of V ($V < 2.405$), only one mode, called the LP_{01} mode, will propagate. Although this mode is doubly degenerate (i.e., two orthogonal polarizations of this mode can simultaneously exist), this region of operation is called single-mode operation.

Generally, one wants a small core radius (typically several wavelengths) and a small index difference (typically less than 1 %) between the core and cladding to achieve this relatively low value of V. For a given fiber geometry, the value of λ that makes V equal to 2.405 is the (theoretical) cutoff wavelength of the fiber. (The actual cutoff wavelength is very susceptible to variations in the fiber parameters and, so, is usually a measured fiber parameter.)

From the power distribution curve at V = 2.405, approximately 84% of the mode's power is in the core while at V = 1, only 30% is in the core and also, about 75% of the power is in the core when V = 2.0. The power in the cladding is at risk to being removed by jacket losses, splices, and other loss mechanisms. For this reason single-mode fibers keep V in the range $2.0 < V < 2.405$. Some compromise is required here. If V is made too close to 2.405, the cutoff wavelength of the fiber will be too close to the designed operating wavelength; if V is made too small, significant cladding power will be removed, raising the optical losses too much.

2.4.3.1.2 Mode Field Diameter

In single-mode fibers, an appreciable part of the wave is contained in the cladding outside of the core. For such waves the use of the core diameter to express the "width" of the wave is no longer possible, since the wave "width" is now larger (or smaller) than the core. The "width" of the wave is an important quantity in predicting the cabling losses, the losses due to bends, and the joining losses when the cables are connected or spliced together.

For single-mode fibers, a useful measure of the field "width" has been the mode field diameter (usually abbreviated "MFD"). If the fiber produces a Gaussian-shaped field, then the definitions all reduce to the same value. [5]

2.4.3.2 Mode coupling

When modes are near to cutoff, a higher proportion of their power propagates in the cladding than is the case for the lower order modes. As a result, those modes having fields, which extend further in to the cladding were highly attenuated, are certainly more susceptible to bending & micro bending effects.

It should be mentioned that a significant number of modes, while they are not fully guided, do nevertheless propagate considerable distances along the fiber. These are known as leaky modes. For them,

$$\beta_c^2 > \beta^2 > \beta_c^2 - \frac{\kappa^2}{a^2} \tag{2.4}$$

they do not satisfy the condition $\beta^2 > \beta_c^2$ & do not constitute fully guided modes. Unwanted higher -order & leaky modes can easily be removed by bending a short length of the fiber in to a tight curve. This has an effect of locally lowering the value of V, the normalized optical frequency, & as a result a no of higher order modes that would be guided or only showily leaky in a straight length of the fiber find themselves below cutoff, so they radiate out in to the cladding. This is sometimes referred to as mode stripping.

2.4.3.3 Cladding Modes and Leaky Modes

As noted in Fig. 2.7 on the preceding page, certain rays in the incident radiation are not captured by the core of the fiber, but pass through the core-cladding interface into the cladding region. Because of the finite radius of curvature of the outer cladding surface, some of this light at this boundary will be reflected back into the cladding, where it can be trapped and propagated. This light forms the cladding modes of the fiber and appreciable coupling can occur with the higher-order modes of the core, resulting in increased loss of the core power. Cladding modes are suppressed by placing a high-loss material outside of the cladding surface that will absorb the light as it strikes the interface by increasing the scattering at the cladding interface to extract the cladding modes, or by surrounding a portion of the fiber with a material whose index of refraction matches that of the cladding, causing the cladding light to transmit into the index matching material (see Fig. 2.8). This latter technique is called mode stripping.

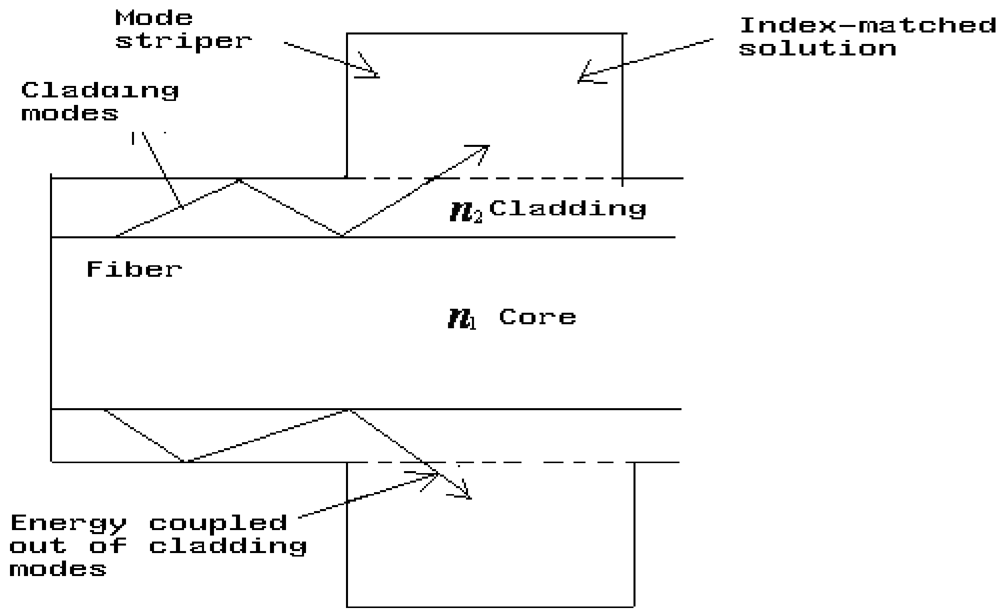

Figure 2.3: Removal of cladding power by a mode stripper

2.4.3.4 Power density distribution

One of the benefits of the mode analysis is that it enables the power density distribution in the fiber for each mode to be derived straight forwardly by evaluating the pointing vector, ExH, for the transverse field over the fiber cross-section. It is then possible to determine the extent to which the electromagnetic wave penetrates the core-cladding interface and spreads in to the cladding the fraction, Γ, of the total power in each mode that is carried in the core can then be evaluated by integrating over the core cross section. As expected, most of the power flow is to be found in the fiber core except when modes are near to cutoff. Even at cutoff, only a fraction $\frac{1}{\kappa}$ of the power in the higher order modes propagates in the cladding.

The situation is different with $SMF_{s.}$ A considerable fraction of the total power may propagate in the cladding layer or layers, and knowledge of the power distribution is necessary in order to minimize splicing and connector losses and to maximize coupling efficiency. The decay of the evanescent fields also affects the vulnerability of the fiber to bending and micro bending losses.

2.4.3.5 Evanescent wave

When light suffers total internal reflection an electromagnetic disturbance, known as an evanescent wave, does penetrate the reflecting interface. The amplitudes of the evanescent fields decay exponentially with distance away from the surface cannot normally propagate in the medium of lower refractive index. However, any variation or non uniformity in the region of the reflecting interface may cause the conversion of the evanescent wave in to a propagating wave.

In the cladding (r>a), the axial field components are given by

$$\psi_Z = \psi_2 K_K(wr)\cos k\phi \tag{2.5}$$

Where ψ_2 is a constant electric or magnetic field; k is again an integer; and w is related to β and, the modified Hankel functions, $K_k(wr)$, decay monotonically to zero. For large values of r such that r > a and wr >>1.

$$K_k(wr) \propto \frac{\exp(-wr)}{(wr)^{\frac{1}{2}}} \tag{2.6}$$

This means that the fields in the cladding die away exponentially at large radial distances from the core-these are the evanescent fields. [12]

2.4.3.6 Gaussian Approximation

The modal field (near-field) of a single mode fiber is not very sensitive to its refractive index profile and the shape of this field remains similar to a Gaussian function. This has led to the so-called Gaussian approximation in which it can approximate the modal field of a given single mode fiber by a Gaussian function as

$$\psi_G(r) = \psi_G(0)\exp\left[-\frac{r^2}{W_G^2}\right] \quad (2.7)$$

where, W_G is called the spot-size (or, more precisely, the Gaussian spot-size) of the modal field. This spot-size is the parameter which is different for different profiles of the fiber and for different V-values for a given profile.

Although there are a number of criteria to obtain the value of W_G for a given fiber at a given V-value, the most popular method is the one suggested, by Marcuse, in the first proposal for this approximation. In this method, the best Gaussian is obtained- by maximizing the overlap integral between the actual modal field and the Gaussian function. This would physically mean that the best Gaussian function corresponds to that Gaussian beam which would couple maximum power to the mode of the given fiber. Marcuse also gave an empirical formula for obtaining the Gaussian spot-size for a fiber with q-profiles; the formula for a step-index fiber is

$$\frac{W_G}{a} = 0.65 + \frac{1.619}{V^{1.5}} + \frac{2.879}{V^6} \quad (2.8)$$

where a is the radius of the core of the fiber. As the V value approaches to 2.2-2.3 there will be a good fit of the Gaussian to the modal field. However, the Gaussian approximation becomes poorer as the V -value becomes smaller. In most practical cases, the parameter of the single mode fibers are chosen such that the V -value is just below the limit of single mode operation (that is, the V-value is just below V_{c11} the cutoff V-value of the next higher mode). Thus, a step-index fiber (V_{c11} = 2.405) is generally operated around V ~ 2.2-2.3 single and the Gaussian approximation can be useful in estimation of its propagation characteristics.

The Gaussian approximation can be used for estimation of those characteristics of the fiber which directly depend on the modal field distribution, such as the source-to-fiber coupling efficiency, splice losses, bending and micro bending losses, etc.

2.4.3.7 Spot Sizes

This section discusses the relationship of spot-size to various characteristics of single mode fibers. Twice the value of a spot-size is sometimes referred to as the mode field diameter (MFD).

The third spot-size W_∞, which is also called the Petermann-3 spot-size, is defined as

$$W_\infty^2 = \frac{\lambda}{\pi n_1(\beta - k_0 n_2)} \cong \left(\frac{2a}{W}\right)^2 \tag{2.9}$$

Where β is the propagation constant of the LP_{01}-mode. This spot-size is related to the bending loss in a fiber.

2.4.3.8 Gaussian Beams

Optical beams change their intensity distribution as they propagate in space. This is due to the phenomenon of diffraction. Diffraction can easily be understood by considering the diffraction divergence of a Gaussian beam. Indeed, when a laser oscillates in its fundamental mode, the transverse amplitude distribution is Gaussian. Similarly, the transverse amplitude distribution of the fundamental mode of an optical fiber is very nearly Gaussian. Therefore, the study of the diffraction of a Gaussian beam is of considerable importance in fiber optics.

Consider Gaussian beam propagating along the z-direction with intensity distribution on the plane z=0 given by

$$I(x, y, 0) = I_O \exp\left[\frac{2(x^2 + y^2)}{w_O^2}\right] = I_O e^{\frac{-2r^2}{w_O^2}} \tag{2.10}$$

Where I_O is the intensity at the beam centre and w_O is a measure of the beam width, usually referred to as the spot-size of the beam; it represents the distance at which the intensity falls off to I_O/e^2. Assume that the phase front is a plane at z=0. As the beam propagates along the axis, diffraction occurs and one obtains the transverse intensity distribution after a propagation distance z as

$$I(x,y,z) = I_O \frac{w_O^2}{w^2(z)} \exp\left[-\frac{2(x^2+y^2)}{w_O^2(z)} \right] = I_O \frac{w_O^2}{w^2(z)} e^{-\frac{2r^2}{w^2(z)}} \tag{2.11}$$

Where $w(z)$ is the z-dependent spot-size of the beam given by

$$w(z) = w_O \left(1 + \frac{\lambda^2 z^2}{\pi^2 w_O^4} \right)^{\frac{1}{2}} \tag{2.12}$$

The above equation implies that w (z) increases with the diffraction divergence of the beam. [13]

2.5 Fiber losses

Light power propagating in a fiber decays exponentially with length due to absorption and scattering losses. Attenuation is the single most important factor determining the cost of fiber optic telecommunication systems as it determines spacing of repeaters needed to maintain acceptable signal levels. In the near infrared and visible regions, the small absorption losses of pure silica are due to tails of absorption bands in the far infrared and ultraviolet. Impurities-notably water in the form of hydroxyl ions-are much more dominant causes of absorption in commercial fibers. Recent improvements in fiber purity have reduced attenuation losses. States-of the-art system can have attenuation on the order of 0.1dB/km. Scattering can couple energy from guided to radiation modes, causing loss of energy from the fiber. There are unavoidable Rayleigh scattering losses from small scale index fluctuations frozen in to the fiber when it solidifies. This produces attenuation proportional to $1/\lambda^4$. Irregularities in the core diameter and geometry or changes in fiber axis direction also cause scattering.

2.5.1 Attenuation

The basic attenuation mechanisms in a fiber are absorption, scattering and radiative losses of the optical energy. Absorption is related to the fiber material, where as scattering is associated both with the fiber material and with structural imperfections in the optical waveguide. Attenuation owing to radiative effects originates from perturbations (both microscopic and macroscopic) of the fiber geometry.

This section discusses the units in which fiber losses are measured and then present the physical phenomenon giving rise to attenuation.

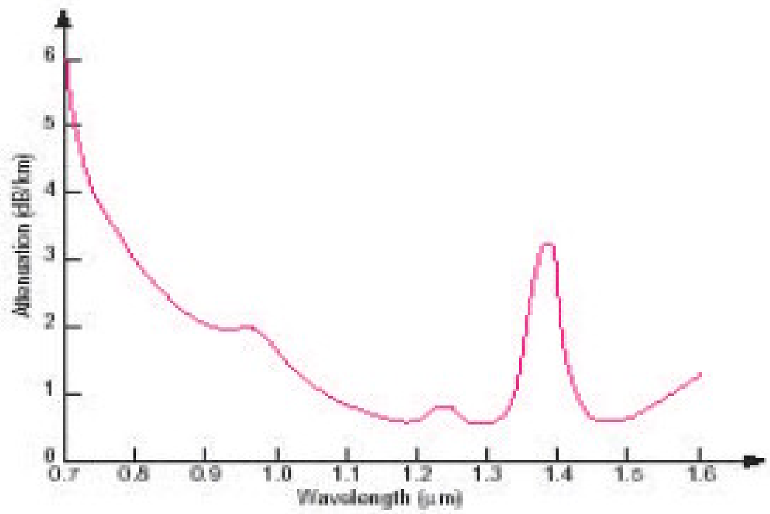

Figure 2.4: Typical spectral attenuation in silica

Fiber losses are due to several effects; among the more important are:

2.5.2 Scattering

By its nature glass is a disordered structure in which there are microscopic variations around the average material density, and local microscopic variations in composition. Each of these gives rise to fluctuations of refractive index on a scale that is small compared to optic wavelength, that is, on a submicron scale. This is fundamental to any glassy material, however carefully made, and it causes the light to be scattered in the manner known as Rayleigh scattering. The light is then lost from the fiber. Indeed, if visible light from a laser is coupled in to a long coil of unsheathed fiber and this is viewed from the side in a darkened room, the scattered light is clearly seen, diminishing in intensity along the length of the fiber.

The loss caused by this mechanism can be minimized by cooling the melt from which the fiber is drawn in as carefully controlled a manner as possible. The loss is likely to be higher in multi component glasses because of compositional variations. Its essential characteristics is that the scattered power, and hence the attenuation, is inversely proportional to the fourth power of the wavelength. Fig 2.5 shows that it is Rayleigh scattering rather than the UV absorption band-edge that is the principal cause of loss in silica fibers at wavelength less than 1.5 μm. For glasses with high silica content, a typical value for the Rayleigh scattering attenuation is 1dB/km at 1 μm. Germania doping usually causes a slight increase and phosphorous pent oxide a slight decrease. This effect can be seen in Fig 5.3 very carefully made single-mode fibers with only a slightly doped core ($\Delta n = 0.003$) can show as little as 0.9 dB/km Rayleigh scattering loss at 1 μm, and in single -mode fibers made with a core of pure silica, this value has been reduced to 0.7dB/km.

In general, a Rayleigh scattering loss coefficient, α_R may be defined such that

$$\alpha_R = A_R / \lambda^4 \tag{2.13}$$

Where A_R is a constant for any given material up to the present tacity assumed that the geometry of any fiber is perfect from end to end and that the fiber itself is straight. In practice, of course, this is not the case and the bends and imperfections that do not occur lead to the guided rays being scattered in the rays, which are radiated away from the core-cladding interface.

Major disturbances to the geometry of this interface (steps, offsets, inclusions) and large imperfections within the fiber core (bubbles, impurities) each give rise to a large local scattering loss. Such imperfections show up quite clearly as locally bright regions when visible light is propagated through an unsheathed fiber. This enables unsatisfactory lengths of fiber to be identified easily and discarded.

Tight bends similarly cause some of the light not to be internally reflected but to propagate in to the cladding and be lost. In theory the optical power scattered out of a fiber at a major bend depends exponentially on the bend radius, R. The bending loss is then proportional to $\exp\left(R/R_C \right)$. At a bend of radius, R_C the loss would be very considerable, but because of the form of the exponential function the losses decrease rapidly for less tight bends. In monomode fibers, vulnerability to bending losses depends on the extent to which the electromagnetic fields penetrate in to the cladding, and hence on the refractive index profile and the wavelength, λ_C.

To understand bending loss, imagine the evanescent fields extending in to the cladding but decaying exponentially with radial distance. Planes of constant phase are roughly perpendicular to the fiber axis. The phase velocity of any guided mode is less than that of plane waves in the cladding, $\frac{c}{n_2}$. But on the outside of a bend, it increases with radial distance, eventually reaching $\frac{c}{n_2}$. The fields beyond this point are no longer guided.[12]

Scattering may be partly a material property, but may also be caused by imperfections in the fiber geometry. It occurs when the mode of propagation of the light is changed such that some of the optical energy leaves the fiber. There is no conversion of the radiant energy in to other forms.

In both cases, the power lost when an optical pulse of energy, E, propagates through a short axial element δz of a fiber is proportional to both ε and δz Thus,

$$-\left(\frac{d\varepsilon}{dz} \right)\delta z = \alpha\varepsilon\delta z \tag{2.14}$$

where α is the attenuation coefficient. When α is independent of z, the energy decays exponentially with distance.

$$\varepsilon(z) = \varepsilon(0)\exp(-\alpha z) \tag{2.15}$$

Traditionally, does not depend only up on the quality of the core material. The cladding material may also be significant. In the process of total internal reflection the electromagnetic fields penetrate the core-cladding interface and extend in to the cladding. Thus, a fraction of the total optical power propagates in the cladding. If the cladding material is of poor quality or is highly absorbing; it contributes to the overall fiber attenuation. Fibers required to have minimal attenuation are made with the inner regions of the cladding material as high in quality and as carefully controlled as the core. It is then necessary to ensure that any light scattered in to the cladding does not propagate and enter the detector, because this is likely to increase the range of propagation velocities and make the fiber dispersion worse. Two steps can be taken to avoid this: the outer layer of the cladding can be made absorbing so that the scattered rays are attenuated there but the propagating light is unaffected; the cladding itself can be surrounded by a protecting polymer layer of higher refractive index in to which the scattered rays pass and are absorbed.

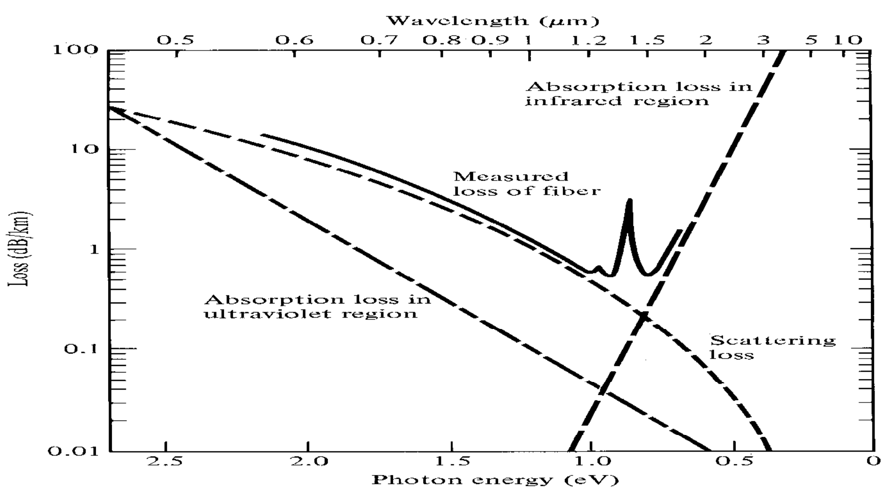

Figure 2.5: Scattering and Absorption losses

2.5.3 Absorptive Losses

In addition to scattering losses, when light passes through a material, it suffers absorptive losses, i.e., a small fraction of its power is absorbed during propagation. These losses may be classified into intrinsic and extrinsic absorption losses.

Intrinsic absorption is caused by the interaction of the propagating waves with one or more major components of glass that constitute the fiber's material composition. An example of such an interaction could be the infrared absorption bands of SiO_2. However, in the wavelength regions of interest to optical fiber communication (0.8-0.9 μm and 1.2-1.5 μm), the infrared absorption tail make a negligible contribution.

On the other hand, extrinsic absorption is caused by the present of minute quantities of materials like transition metal ions (e.g., Fe^{++}, Cu^{++}, Cr^{+++}, etc.) and due to OH^- ions in glass. For example the presence of 1 ppm (part per million) of Cu^{++} would lead to a loss of 1.1 dB/km at λ =0.85 μm. This makes it mandatory to use ultra pure raw materials in the manufacturing of fibers. The technology today has almost eliminated these losses and the total loss in fibers has reached the minimum expected from scattering losses. The presence of OH^- ions leads to absorption peaks at about 0.72, 0.88, 0.95, 1.13, 1.24 and 1.38 μm wavelengths. The prominent peaks at 1.24 and 1.38 μm in Fig.2.4 are due to the presence of OH^- ions. Fortunately these absorption bands are narrow enough so that ultra pure fiber exhibit losses <0.2 dB/km at λ =1.55 μm. Fig.2.4 shows that loss curve has minima at around λ = 1.3 μm and 1.55 μm. These low loss regions are generally referred to as the second and the third low loss windows.

The electronic and atomic resonances which are responsible for dispersive properties of a dielectric material also give rise to absorption in the vicinity of the resonance frequencies. These are resonances in the ultra-violet associated with the band-gap of the material and the electronic structures of the crystal atoms, and resonances in the infra-red associated with the lattice vibrations of the atoms themselves. Although these resonance frequencies are well away from the optical frequencies, the absorption they produce is very strong and the tails of their absorption bands do extend in to this region at the very low levels of attenuation.

In general, such absorption band-edges show an exponential variation of the absorption coefficient with photon energy. Thus, the absorption coefficient associated with the UV band-edge, α_{UV}, may be expressed as

$$\alpha_{UV} = A_{UV}\exp\left(\frac{\varepsilon}{\varepsilon_{UV}}\right) = A_{UV}\exp\left(\frac{\lambda_{UV}}{\lambda}\right) \quad (2.16)$$

where A_{UV} , ε_{UV} and λ_{UV} are constants. This relationship is usually called the Urbach law, although the exact reasons for it are not fully understood. The absorption coefficient associated with the infra-red band-edge may likewise be expressed as:

$$\alpha_{ir} = A_{ir} \exp\left(\varepsilon / \varepsilon_{ir} \right) = A_{ir} \exp\left(\frac{\lambda_{ir}}{\lambda} \right) \qquad (2.17)$$

Again, A_{UV}, ε_{ir} and λ_{ir} are constants.

Superimposed on the IR band edge are absorption peaks associated with harmonics of the fundamental frequencies.

An estimate of the attenuation produced by the absorption band-edges in silica is shown in Fig.2.5. Values of the constants can be estimated from the diagram .The window between the two edges should be greatest at about 1.5 μm, but it is considerably reduced because another fundamental loss mechanism dominates the UV absorption band-edge at wavelengths longer than about 0.3 μm. This is Rayleigh scattering.

The IR band-edge becomes significant at wavelengths longer than 1.5 μm. This edge is associated with the characteristics stretching vibrations of the oxide bonds. These have the following fundamental resonance frequencies:

Si - O	9.0 μm
Ge - O	11.0 μm
P - O	8.0 μm
B - O	7.3 μm

From this point of view germania should be the most favorable impurity because of the longer wavelength associated with the Ge-O stretching vibration.

The band-edge absorption is inherent in the material used to make the fiber. However, this material may also contain impurity atoms and molecules which can cause absorption at wavelengths of interest. In practice, it is found that hydroxyl ions, hydrogen and the first row of transition metals (vanadium, chromium, Manganese, Iron, Cobalt and Nickel) are the most precious of these. The metals occur in the glass as ions, which by virtue of their electronic structure give rise to broad-band absorption at wavelengths which may depend up on the state of oxidation of the ion. As a very approximate indication, the concentrations of these transition-metal ionic impurities have to be kept below about 1 part in 10^9 for their contribution to absorption not to exceed 1dB/km at wavelengths in the region of 1 μm.

The absorption caused by hydroxyl ions arises from the basic stretching vibration of the O-H bond. Its fundamental frequency, f_s is centered at 2.73 μm but it gives rise to harmonics and to combination frequencies with the Si-O bonding resonance at 12.5 μm [13].

2.5.3 Radiation losses in optical fiber

Optical energy can be lost form waveguide modes by radiation, in which case photons are emitted in to the media surrounding the waveguide and are no longer guided. Radiation can occur from planar waveguides as well as from channel waveguides.

2.5.3.1 Radiation loss from planar and straight Channel Waveguides

Radiation losses from either planar or straight channel waveguides are generally negligible for well confined modes that are far from cutoff. However, at cutoff, all of the energy is transferred to the substrate radiation modes. Since the higher-order modes of a waveguides are always either beyond cutoff or are, at least, closer to cutoff than the lower-order modes, radiation loss is greater for higher-order modes. In an ideal waveguide the modes are orthogonal, so that no energy will be coupled from lower-order modes to the higher-order modes. However, waveguide irregularities and inhomogeneities can cause mode conversion, so that energy is coupled from lower-order to higher-order modes. In that case, even though a particular mode may be well confined, it may suffer energy loss through coupling to higher-order modes with subsequent radiation. This problem is not usually encountered in typical waveguides of reasonably good quality, and radiation losses can generally be neglected compared to scattering and absorption losses. The one important exception is the case of the curved channel waveguides.

2.5.3.2 Radiation loss from Curved Channel Waveguides

Because of distortions of the optical field that occurs when guided wave travel through a bend in a channel waveguide, radiation loss can be greatly increased. In fact, the minimum allowable radius of curvature of a waveguide is generally limited by radiation losses rather than by fabrication tolerances. Since waveguide bends are a necessary part of all but the simplest OIC's the radiation losses from a curved waveguide must be considered in circuit design.

A convenient way of analyzing radiation loss is the velocity approach developed by Marcatili and Miller [14]. The tangential phase velocity of waves in a curved waveguide must be proportional to the distance from the center of curvature because otherwise the phase front would not be preserved. To appreciate this, consider the case of a waveguide mode assumed to be propagating in a circular bend of radius R, with a propagation constant $ß_z$. There is a certain radius (R+Xr) beyond which the phase velocity would have to exceed the velocity of unguided light (in the confining medium, with index n1), in order to preserve the phase front. Since $\frac{d}{dt}$ must be the same for all waves along the phase front, two resultant equalities are that

$$(R+Xr)\frac{d\theta}{dt}=\frac{\omega}{\beta_o} \tag{2.18}$$

And

$$R\frac{d\theta}{dt}=\frac{\omega}{\beta_O} \tag{2.19}$$

Where β_o is the propagation constant of unguided light in medium 1, and $ß_z$ is the propagation constant in the waveguide at radius R.

Combining eqn.(2.18) & (2.19) leads to

$$X_r = \frac{\beta_z - \beta_o}{\beta_o} R$$

The radiation process can be visualized as follows. Photons of the optical mode located at radii greater than R+X_r cannot be travel fast enough to keep up with the rest of the mode. As a result, they split away and are radiated in to Medium 1. [15]

2.5.3.1 Bending Loss in Optical Fiber

A bend in a fiber can be considered to be a straight fiber section joined with a bent fiber section, which is again jointed with a straight fiber as shown in Fig. 2.6. The power from the straight fiber is coupled to the field in the bent fiber. The field in the bent fiber propagates through to be coupled into the following straight section. Thus, there are transition losses at the joints and there is loss in the curved fiber section generally termed as pure bend loss. For a bent fiber as shown in

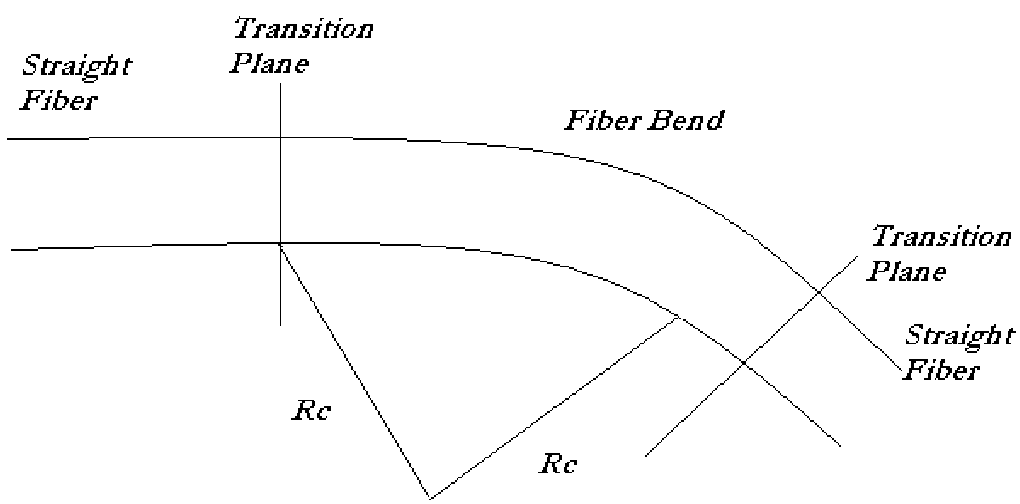

Figure 2.6: Schematic showing the geometry of a fiber bend

bend alone and two contributions from transitions at the ends of the bend. In a bent fiber, the field launched from the mode of the straight fiber does not propagate as a mode and the field distribution changes substantially. One important change is that the field no longer has a maximum at the fiber axis and it shifts slightly in the direction away from the center of curvature of the fiber bend (see Fig.2.7). This shift is rather difficult to obtain exactly, but using the Gaussian approximation of the fields, a simple expression has been obtained

$$d_c = \frac{\beta^2 W_G^4}{2R_c} \tag{2.20}$$

where β is the propagation constant of the mode in the straight waveguide, R_c is the radius of curvature of the bend and W_G is the Gaussian spot-size. Thus, at the transition, there is effectively a transverse offset in the fields and the loss can be modeled.

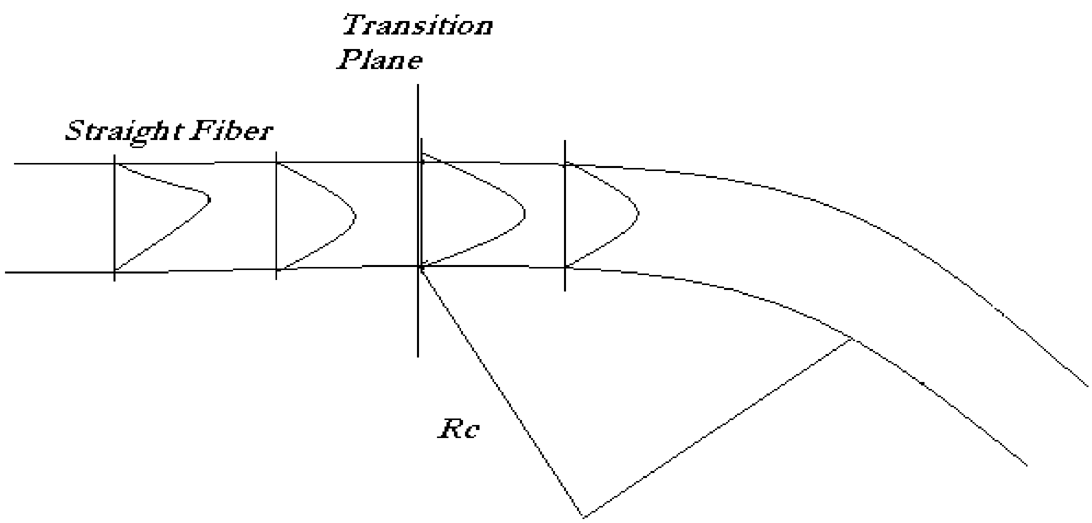

Figure 2.7: Schematic showing shift of the peak of the field away from the center of curvature of the fiber

The pure bend loss coefficient in a step-index fiber is given by

$$\gamma_C = \left(\frac{\pi}{4a R_C}\right)^{\frac{1}{2}} \left(\frac{U}{V K_1(W)}\right)^{\frac{1}{2}} \frac{1}{W^{\frac{3}{2}}} \exp\left[-\frac{2W^3}{3k_0^2 a^3 n_1^2} R_c\right] \tag{2.21}$$

Where n_1 is the refractive index of the core and $U = a(k_0^2 n_1^2 - \beta^2)^{\frac{1}{2}}$ and $W = a(\beta^2 - k_0^2 n_2^2)^{\frac{1}{2}}$. Using the definition given in Eq. (2.13), the above expression can be expressed in terms of the spot-size, W_∞. Thus, the loss coefficient (per unit length) of the bent fiber is given by

$$\gamma_c = \left(\frac{\pi}{32}\right)^{\frac{1}{2}} \left(\frac{U}{V K_1(W)}\right)^2 \left(\frac{W_\infty^3}{a^4 R_c}\right)^{\frac{1}{2}} \exp\left[-\frac{4\lambda^2}{3\pi^2 W_\infty^3 n_1^2} R_c\right] \quad (2.22)$$

It should be noted that in evaluating the above expression all the quantities λ, W_∞, a and R_C must have the same units, e.g., μm, nm The unit of γ_C would then be inverse of that length unit and the loss (fractional) of a length of fiber could be obtained by multiplying the length (in the same length unit) by γ_C. The loss in dB per unit length would be given by

$$\alpha = 4.343\,\gamma_C \quad (2.23)$$

As λ increases, the spot-size becomes larger and the bend loss increases. In the figure, it has been assumed that the LP_{11}-mode cutoff wavelength is 1.2 μm, which represents the lower limit of the wavelength for single mode operation of the fiber.

Bend losses are particularly important in single-mode fiber. In these fibers, the bend losses show a dramatic increase above a critical wavelength when the fiber is bent or perturbed. In particular it has been observed that the bend losses can be appreciably high at 1550 nm in fibers designed for operation at 1300 nm [16]. The susceptibility of a fiber to these losses depends on the MFD and the cutoff wavelength [12, 13-15]. In general, the worst-case condition is in a fiber with a large mode-field diameter and low cutoff wavelength. Bending losses are minimized in single-mode fibers by avoiding this combination of features.

Optical fibers need to be bent for various reason both when deployed in the field and particularly within equipment. Bending leads to “leakage” of power out of the fiber core in to the cladding, resulting in additional loss. A bend is characterized by the bend radius –the radius of curvature of the bend (radius of circle whose arc approximates the bend). The” tighter” the bend, the smaller the bend radius and the larger the loss. The bend radius must be of the order of a few centimeters in order to keep the bending loss low.

Also, the bending loss at 1550nm is higher at 1310nm. The ITU-T standards specify that the additional loss at 1550nm due to bending must be in the range 0.5-1dB, depending on the fiber type, for 100turns of fiber wound with a radius of 37.5mm. Thus, a bend with a radius of 4cm results in a bending loss of <0.01dB. However, the loss increases rapidly as the bend radius is reduced, so that care must be taken to avoid sharp bends, especially within the equipment.[5]

Fibers show increased losses due to bending effects [11-14]. Large bends of the cable and fiber are macrobends;

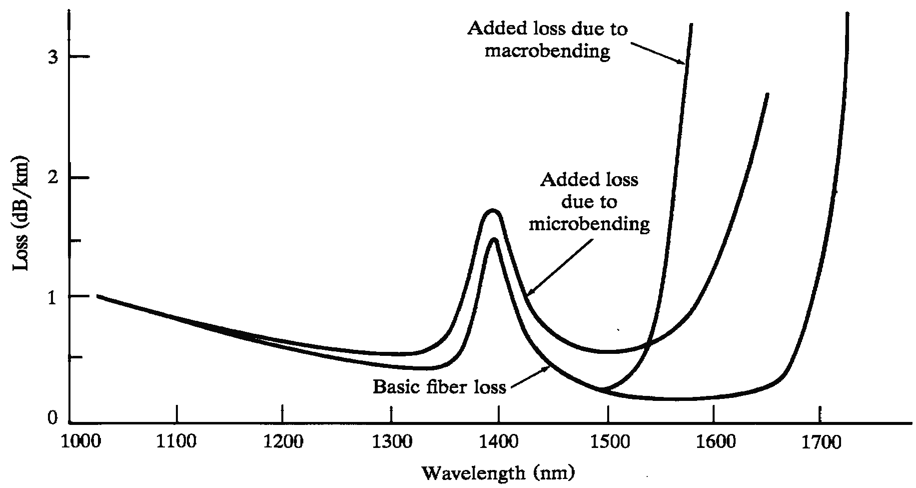

Figure 2.8: An extra loss due to microbending and macrobending on the basic fiber loss

Radiation losses occur at bends in the fiber path. At a bend, the geometry of the core-cladding interface changes and some of the guided light is transmitted from the core in to the cladding-the lower -order modes. The radius of curvature of fiber bend is critical to the amount of power lost.

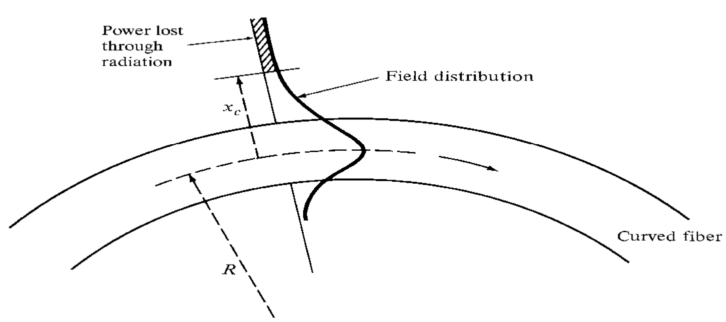

Figure 2.9: Power lost and field distribution in a bend fiber

The loss coefficient associated with a fiber bend is given by [17]

$$\frac{P_{out}}{P_{in}} = e^{-\alpha z} \tag{2.24}$$

and the attenuation coefficient α_{bends} is also given by [17]

$$\alpha_{bends} = c_1 e^{-c_2\, r} \tag{2.25}$$

Where r is the radius of curvature of the fiber bend and c_1 and c_2 are constants. The losses are negligible until the radius reaches a critical size given by [15]

$$r_{critical} \approx \frac{3 n_2 \lambda}{4\pi (NA)^3} \tag{2.26}$$

From this it is possible to minimize these losses, using a fiber with a large NA and to operate at a short wavelength.

Fortunately, macro bending does not cause appreciable losses until the radius of curvature of the bend is below (approximately) 1cm. This requirement does not present much problem in the practical utilization of fiber cables, but does present a minimum curvature to the fiber. Frequently the fiber jacket is stiffened to prevent an attempt to loop the fiber into too small a curvature.

As the curvature of the bend is much larger than fiber diameter, Light wave suffers sever loss due to radiation of the evanescent field in the cladding region. As the radius of the curvature decreases, the loss increases exponentially until it reaches at a certain critical radius. For any radius a bit smaller than this point, the losses suddenly become extremely large. Higher order modes radiate away faster than lower order modes.

3. METHOD AND MATERIALS

3.1 Materials

The materials and equipments used in the entire experiment of this thesis are the following:

3.1.1 Light source

- 1mW He-Ne laser
- 25W Mercury Vapor Lamp

3.1.2 Equipment

- 0.7mm light source circular aperture
- 0.5mm light source aperture
- 18mm focal length convex lens
- 48mm focal length convex lens
- Collimating lenses
- 50% beam splitter
- Photometer
- Flat surface mirror
- Bending apparatus

3.1.3 One meter length fiber

3.2 Method

The method applied to this thesis throughout the experiment is beam-optic launch type. A beam of light is launched through 0.07 apertures and 18mm and 48 mm focal length of lenses and splits by a 50% beam splitter. A portion of the transmitted light passes directly in to the power detector and the other partial power in a fiber of length 1m. The experiment is limited to the range of the visible and ultraviolet region. Two different light sources are introduced:

1) Mercury vapor lamp which has five visible colors, yellow, green, blue and two different violet colors corresponding to wavelengths 578, 546, 436, 405, 366nm

respectively and

2) He-Ne laser of a monochromatic red light of wavelength of 632.8nm.

3.2.1 Measurements using He-Ne laser (without macrobend loss)

In this method, He-Ne laser of 1mW light source is providing a monochromatic red light wavelength equal to 632.8nm passes through 1m length of the fiber (see Figure 3.1.) By using a 0.7mm light source aperture the spot size of the laser is then reduced to lesser diameter. To avoid losses through divergence of spot, light is collimated through 18mm and 48mm focal length convex lenses respectively. Then, it passed through another 0.7mm light source aperture to perfectly lessen its spot. As the launched Light passes through a 50 % beam splitter, it splits in to two paths. The light path collinear to the original laser source is directly recorded to the first photometer as I_i, later regarded as the input power, whereas, the other partial light path passes through the fiber and recorded as I_o. As shown in Figure 3.1.

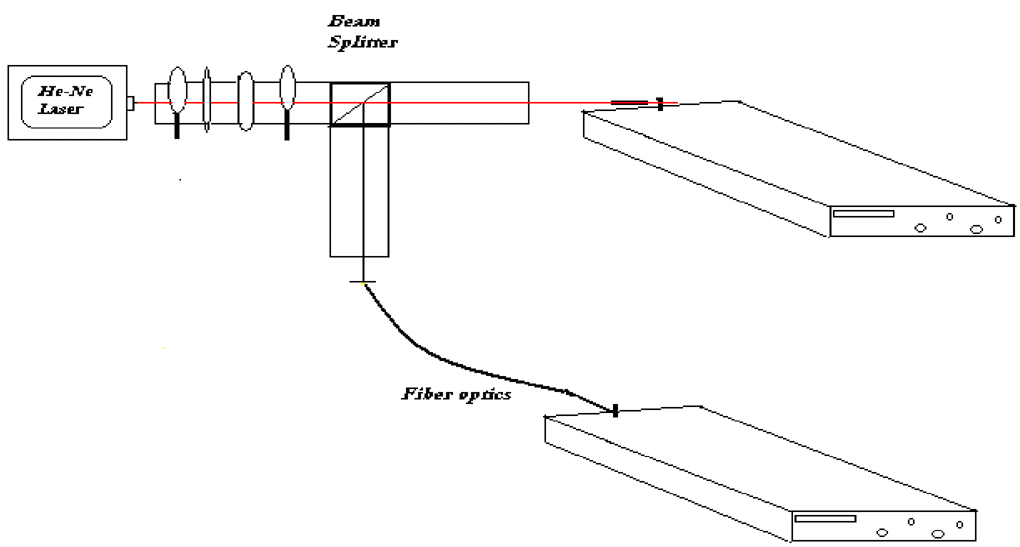

Figure 3.1: Set up for He-Ne laser

3.2.2 Measurements using Mercury Vapor Lamp (Without macrobend loss)

The same method is employed, but here Mercury vapor lamp which has five visible colors but the green one corresponding to wavelengths 546nm are launched. A 0.5mm light source aperture and the collimating lenses are used to focus the light and then using a 50% beam-splitter the in put intensity from the Mercury Vapor Lamp is recorded as I_i and the intensity through the fiber is I_o, as the output intensity using photometer. [See figure 3.2]

3.2.3 Measurements for macrobending loss

Same procedure and methodology is applied as in the case of a straight fiber using both He-Ne laser and mercury vapor lamp light source. The only difference in the case of a bend fiber is using the bending apparatus (refer to Figure 3.2). Here, by varying the bend radius of the fiber output intensity, I_o is recorded for each of the wavelength and then the loss of the fiber (or the bend loss) is calculated as follows.

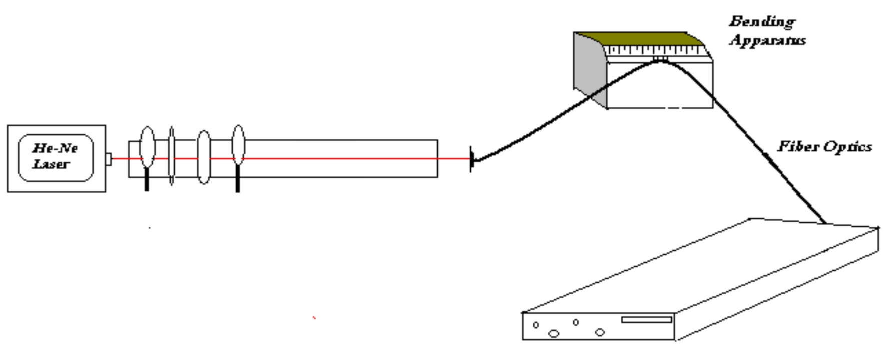

Figure 3.2: Set up for He-Ne laser for the Macrobending

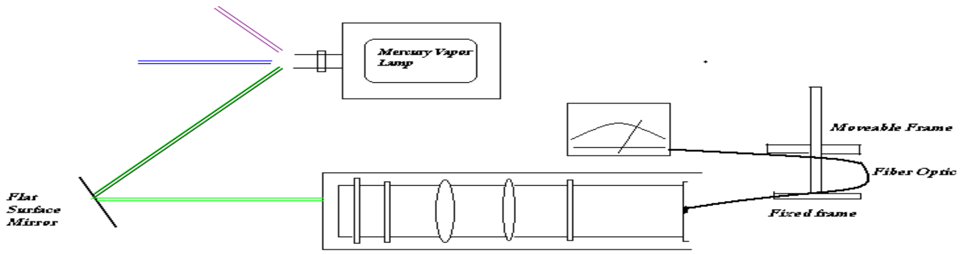

Figure 3.3: Set up for Mercury Vapor for the Macrobending

3.2.4 Theoretical Calculations of fiber bend loss

Total loss of a bent fiber includes the pure bend loss in the bent section and the transition loss caused by the mismatch of propagation mode between the bent and the straight sections. For a single mode bent fiber of length L, the pure bend loss can be calculated by

$$Ls=10\ \log_{10}(\exp(2aL))=8.686\ aL$$

Where a is the so-called bend loss coefficient, which is determined by the fiber structure, bending radius and wavelength of the light. Most theoretical investigations on fiber bend losses are focused on calculations of this bend loss coefficient.

The change in power due to attenuation at a given length of a fiber is defined by

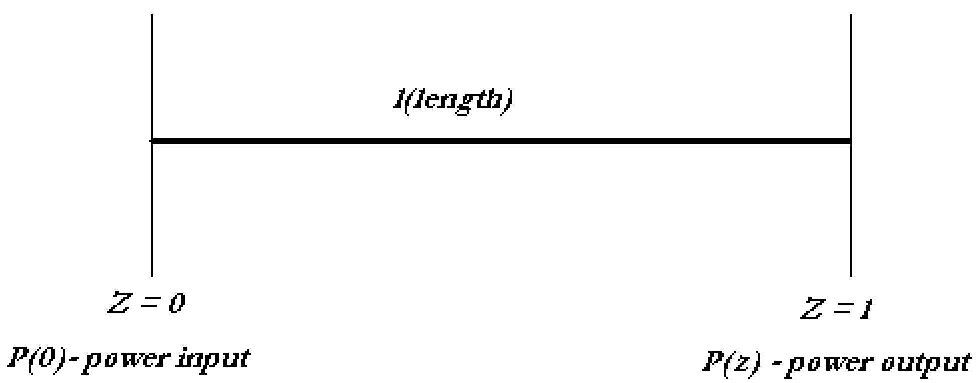

$$\frac{dP}{dZ} = -\alpha P$$

$$\frac{dP}{P} = -\alpha dz$$

$$\left.\frac{dP}{P}\right|_{P(0)}^{P(z)} = -\left.\alpha dz\right|_{z=0}^{z=l}$$

$$\ln p(z) - \ln p(0) = -\alpha l$$

$$\alpha_p = -\frac{1}{l}\ln\left(\frac{p(z)}{p(0)}\right)$$

$$p(z) = p(0)e^{-\alpha_p l}$$

$$\alpha = \frac{-10}{l}\log\left(\frac{p(z)}{p(0)}\right) \equiv \frac{p_{out}}{p_{in}} = 10^{\frac{-\alpha l}{10}}$$

Attenuation [3] is conventionally measured in decibels. If the transmittance of the fiber is T, then attenuation A may be expressed as

$$A = -\log T$$

Attenuation coefficient α is obtained through

$$\alpha = \frac{A}{L} = \frac{-\log T}{L}$$

where $T = \frac{P_{out}}{P_{in}}$ and P_{out} =power output measured, P_{in} = power input measured, and L =length of the fiber optic thus, $\alpha = \frac{-10}{L}\log\frac{P_{out}}{P_{in}}$.

One of the specific aims of this thesis is to obtain the relationship between constant C_α and $-C_R$ against the wavelength. Manipulating bend loss equation (2.1), where $-C_R$ is the slope and c_α is the y-intercept. A graph is drawn for ln α (attenuation coefficient) versus radius of curvature and therefore, constants C_α and C_R will be checked whether it is affected by light source wavelength.

4. RESULT AND DISCUSSION

4.1 Measurement without macrobending

When there is no macro bending in the fiber, the attenuation of the fiber is associated with Rayleigh scattering. Light at shorter wavelengths (or higher frequency) is attenuated more. It coincides with the theoretical Rayleigh scattering.

Theoretically, increasing the light wavelength decreases the amount of Rayleigh scattering, $\alpha_R = A_R/\lambda^4$. As the wavelength increases, the scattering loss decreases which coincides with the theoretical Rayleigh scattering. In other words, its essential characteristics is that the scattered power, and hence the attenuation is inversely proportional to the fourth power of the wavelength. There is high power loss in the visible region, that is, there is an inverse variation of attenuation with an increase in wavelength.

As light source is launched in to the fiber it undergoes an increase in the output intensity and these output intensities increase with increasing of the wavelength but the loss decreases. That means, as the radius, R approaches to the radius of curvature, R_c and when R_c becomes equal to R, then it attains minimum bend loss and the loss will be negligible beyond R_c. In other words, the evanescent wave will be confined to the core region. That is, the loss is not due to bending rather it is due to the intrinsic nature of the fiber.

$\lambda(nm)$	$I_i(a.u)$	$I_0(a.u)$	$\alpha\left(dB/m\right)$
Mercury Vapor Lamp (366-578)	25W	24.8677	2.26×10^{-2}
633	5×10^{-4}W	4.9891×10^{-4}	0.95×10^{-2}

Table 4.1: Loss without macrobending

As the wavelength of the source is increasing, the output intensity decreases in the same trend; however, the loss declines inversely with it. Hence, the experimental values obtained in this thesis work are in a good agreement with the theoretical expectation.

Even if the fiber is straight, there is a loss but this loss is not due to bending rather it is the minimum expected loss in the manufacturing stage (or the intrinsic nature of the fiber).

From Table 4.1 as the wavelength approaches to the UV region, there is a dramatic increment in the loss but it is observed that an extremely low loss at the edge of visible region. Here λ=546nm is used from the other wavelengths of Mercury Vapor Lamp, because its output intensity is stronger than others. in which the loss belongs most probabily to the intrinsic nature of the fiber than bending.

As the wavelength increases, the loss decays exponentially. Even though, there is no loss due to bending, there is a loss which is associated to the theoretical Rayleigh scattering. Light at shorter wavelength particularly when it approaches to ultraviolet region, it attenuates, which is in good agreement with the theoretical Rayleigh scattering and the dominant cause of loss at this ultraviolet region.

4.2 Measurement with macrobending

As you can see from Fig 4.1, the attenuation increases as the bending radius decreases but the attenuation is steady (or remains constant) after a certain critical point, although the bend radius of curvature increases. This point at which $R=R_c=1$ and on wards there is a loss according to the graph. But, it is not due to bending rather it is mostly the intrinsic nature of the fiber (or the expected loss in the manufacturing process) ,that is, it is the case where scattering, absorption and other loss mechanism rather than macrobending.

As can be noticed from Table 4.1, the attenuation is smaller for the large wavelength, 632.8nm in comparison with other wavelengths of the same light source. There is directionality, focusbility and monochromaticity in the He-Ne laser which is far closer to the input intensity than mercury vapor lamp.

R(cm)	a@546nm	a@633nm
0.7	1.4097	1.1984
0.8	1.3840	1.1531
0.9	1.3587	1.1096
1.0	1.3341	1.0677
1.1	1.3121	1.0272
1.2	1.2916	0.9886
1.3	1.2830	0.9732
1.4	1.2715	0.9512

Table 4.2: Bend Loss due to bending for different wavelength

As it can be observed from Table 4.2, the attenuation decreases as the bending radius of curvature increases. As the fiber is tight, its loss is extremely high. Thus, the loss becomes too low in the case of λ=633nm of the He-Ne laser than λ=546nm (green line) of the mercury vapor lamp.

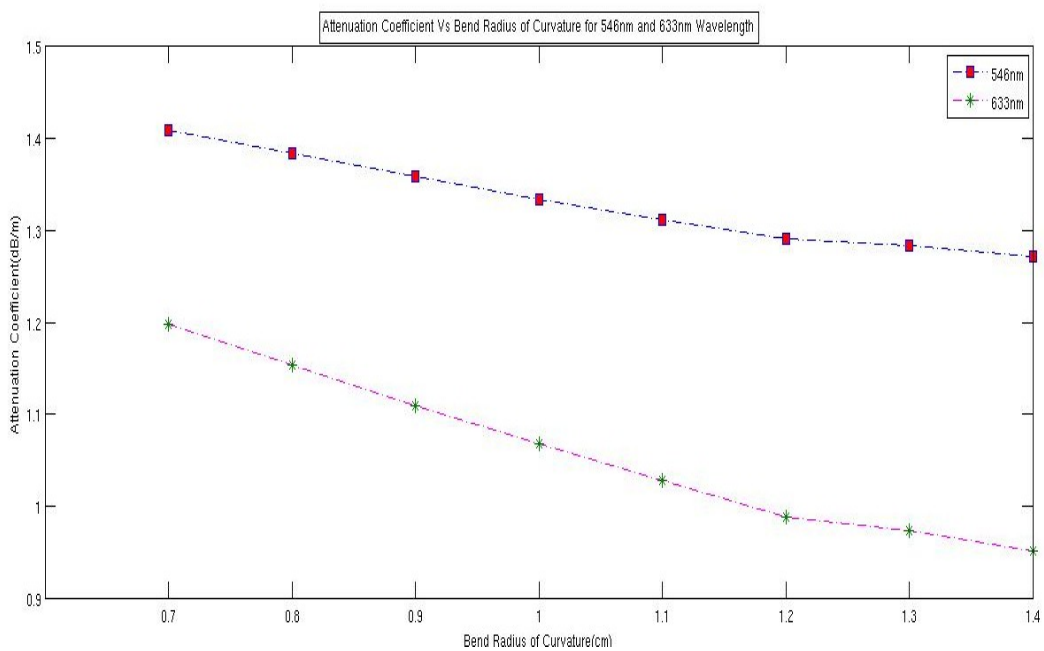

Figure 4.1: Attenuation Coefficient Vs Bend Radius of Curvature

As the bending curvature increases, the loss due to bending rises exponentially

The attenuation value decreases with the increasing wavelength, which is due to a decrease in the curvature of radius. And from the graph there is a point where attenuation becomes constant. This the case where the only dominating loss is scattering, absorption and other loss mechanism excluding macro bending state.

The loss as a consequence of macrobending is extremely low as in the case of high wavelengths, which is, in the case of 633nm. But, the loss is somewhat high for 546nm. From the graph as the wavelength increases the c_R and c_α also increases. This can be mathematically expressed as: $c_R \propto \frac{1}{R_C}$. As the R_C decreases the C_R increases in which the slope in the equation:

$$\ln\alpha = -c_R R + \ln c_\alpha$$

also increases and the attenuation increases. Thus, the difference of the slopes and the intercepts at different wavelengths corresponds to the dependence of constants c_R and c_α to the wavelengths.

R(cm)	$I_i(a.u)$	$I_0(a.u)$	$\alpha(dB/m)$	$\ln\alpha$
0.7	25W	3.9596 x 10^{-4}W	1.1984	0.1809
0.8		3.9466 x 10^{-4}W	1.1531	0.1424
0.9		3.9102 x 10^{-4}W	1.1096	0.1039
1.0		3.8726 x 10^{-4}W	1.0677	0.0652
1.1		3.8340 x 10^{-4}W	1.0272	0.0268
1.2		3.7943 x 10^{-4}W	0.9886	-0.0115
1.3		3.7537 x 10^{-4}W	0.9732	-0.0271
1.4		3.7117 x 10^{-4}W	0.9512	-0.0500

Table 4.3: Bend Loss due to bend Radius of Curvature for λ=633nm

As the bend radius of curvature decreases, the bend loss increases and becomes more significant to the contribution of the basic fiber loss. However, there is a little bit variation in the loss after certain bend curvature, that is, from 1cm on the bend loss is insignificant and from the corresponding $\ln\alpha$ values it is clearly seen that the loss exponentially decays. Figures 4.2 and 4.3 is $\ln\alpha$ vs bend radius for λ= 633nm (red) and λ=546nm (green) respectively. The difference of the slopes and y-intercepts at different wavelengths corresponds to the dependence of constants C_R and C_α to the wavelength.

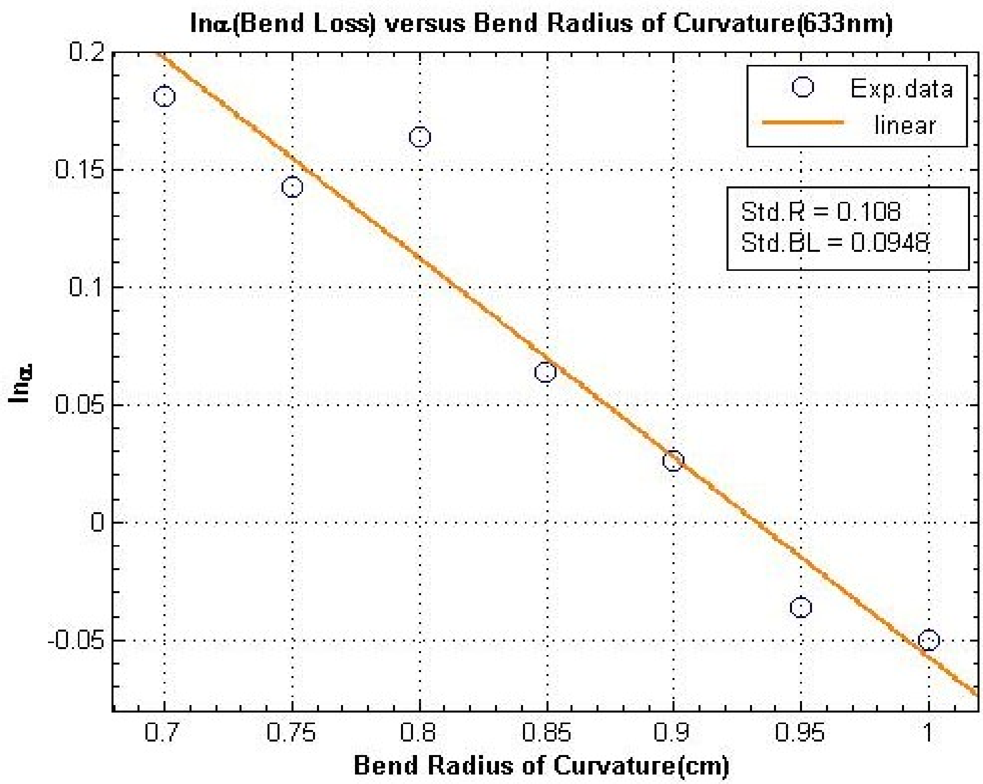

Figure 4.2: Bend loss vs. Bend Radius of Curvature for λ=633nm

The loss at the critical radius is 0.05dB/m. But, in general the power loss due to macrobending decreases as the bend radius of curvature increases.

R(cm)	$I_i(a.u)$	$I_0(a.u)$	$\alpha\left(dB/m\right)$	$\ln\alpha$
0.7	25W	18.5686	1.4097	0.3433
0.8		18.4811	1.3840	0.3250
0.9		18.3878	1.3587	0.3066
1.0		18.2839	1.3341	0.2883
1.1		18.1777	1.3121	0.2717
1.2		18.0704	1.2916	0.2559
1.3		17.8669	1.2812	0.2483
1.4		17.6583	1.2715	0.2402

Table 4.4: Bend Loss due to Bend Radius of Curvature for λ=546nm

From the above table the bend loss at the critical is 1.3341dB/m which is nearly equivalent with for λ = 633nm.

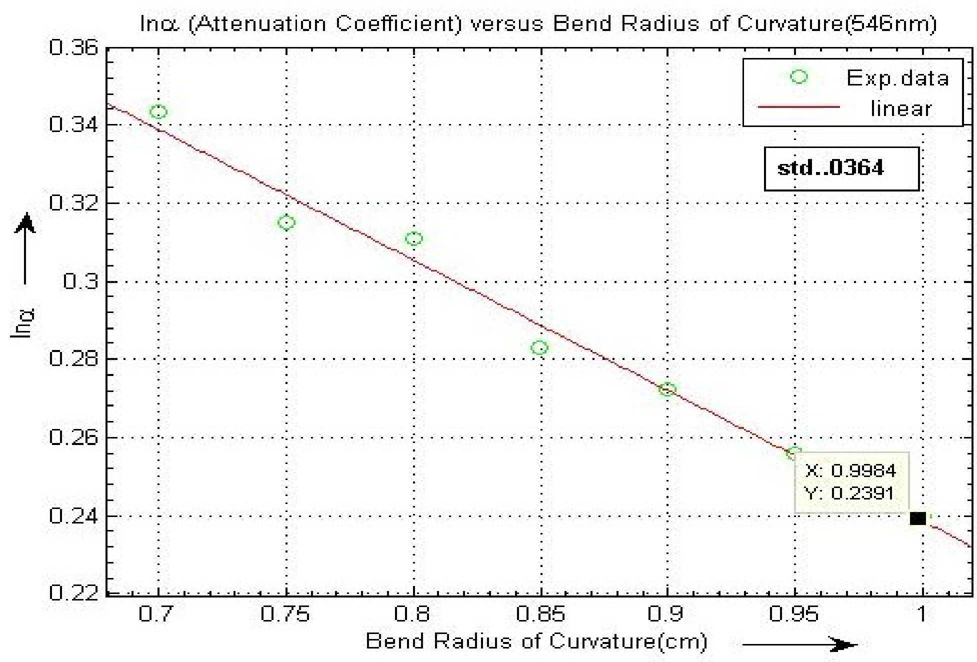

Figure 4.3: Bend Loss vs. Radius of Curvature for λ = 546nm

The attenuation coefficient becomes 0.2398dB/m which shows a dramatic change in the loss at λ = 546nm

$\lambda(nm)$	C_R	C_α	α
546nm	0.3440	1.7933	1.4097
633nm	0.7696	2.0536	1.1984

Table 4.5: The dependence of C_R and C_α with the variation of the different wavelengths

As seen from the above table, the C_R values increase as the wavelength increases. However, C_α seems to decrease smoothly but there is a little bit variation at the higher wavelength. According to table 4.5, the loss is decreasing as it goes down to the higher wavelengths..

The Ca value varies greatly with the shorter wavelength but much smaller for the longer wavelengths. That is, Ca constant depends on the dimension of the waveguide, and on the shape of the optical mode. Here Ca showed a great dramatic variation with the wavelength.

The C_R value abruptly changes for a large wavelength value. So, it can be noted that there is a dependency of C_R with the variation of the different wavelength in which the experimental data are in good agreement with the predicted values.

There is high loss as the bend radius of curvature increases in all the above wavelengths. But, the power loss decays exponentially when the fiber is less and less tightly held. More over, as to the above table suggests the loss due to macrobending is worst in the UV region.

4.3 Data Error Analysis

There are many errors sources in power loss measurement. Those errors might be due to:

- Good coupling efficiency requires precise positioning of the fiber to the center the core in the focused laser beam. Since single mode fibers have got small core size, they require more elaborate couplers with submicron positioning resolution of $\pm 5\,\mu m$. The focused spot could not be comparable to the core size. This is due to the numerical aperture (NA) used in the experiment is not as small as the NA of the fiber.

- Fluctuations in detected power
- The dependence of the detector responsivity on the wavelength and direction of the incident light, and on the ambient temperature; the uniformity of the reponsivity; and the effects of the coupling in to the detector.
- Calibration of the detector and experimental setup
- Coupling effects such as multiple reflections. Even so, a measurement accuracy of ±5% to ±10% is all that can be expected in general.
- The uncertainty of the power measured by the power detector is ±0.0001.

5. CONCLUSION

In this thesis work a 1m length of a single mode fiber from telecommunication is used to characterize the macrobending loss of the fiber. The method used in this experimental investigation is efficient enough to determine the spectral window and the operating wavelength in which a fiber can effectively operates. It also plays a crucial role during installation of the fiber which depends quite a lot on the bending radius so that cost minimization can be made.

As one can see from Table 4.5, it shows the dependence of the constants, C_R, C_a and the attenuation coefficient on the wavelength of light. As the wavelength approaches more to the end of the visible spectrum C_R and C_a also rises but shows a little bit variation, however, the attenuation coefficient declines. This result coincides with the theoretical Rayleigh scattering. Generally, there is a variation of C_R and C_a which shows its dependency on the wavelengths, which are considered in this thesis work.

Further more, it is possible to predict macrobending from the trend of shorter wavelengths that it is minimum at long wavelength.

As a whole the results from the experiment have suggested that the optical power loss due to bending at the visible spectrum is more apparent than loss due to other effects such as absorption and scattering.

The loss of the fiber without macrobending is found to be $0.95x10^{-2}$dB for λ=633nm for He-Ne laser and $2.26x10^{-2}$ for λ=546nm for the mercury vapor lamp which is considered to be the intrinsic nature of the fiber for each of the wavelength. But, when it bends at 1cm radius of curvature it is 1.07dB for λ=633nm and 1.3121dB for λ=546nm where there is a visible difference of loss about 0.242dB between Mercury Vapor Lamp of 546nm and He-Ne laser of 633nm. Thus, there is a considerable bend loss difference for a straight and a bend fiber for different wavelengths and source of light. Hence, it is possible to predict the bend loss at a wavelength of interest using this experimental technique.

The paper confirms how macrobending give rise to a significant loss and important to characterize it. Thus, it is pretty important to consider it and minimize this loss for a better signal transmission.

6. REFERENCE

[1] Max Ming-Kang Liu, "Principles and applications of Optical Communications," McGraw-Hill, New York, 1996

[2] Chen, Chin Lin, "Elements of Optoelectronics and Fiber Optics,'' IRWIN, Chicago 1996.

[3] Gloge, Detlef, "Optical Fiber Technology," IEEE Press, Newyork, c1976

[4] Deutsch, Bernhard and David R. Velasquez. "Bending over backwards'' Corning. Aug.2007.OSP.30Nov.2007<http://www.corning.com\docs.\clearcurve\EVO_757_ bend%20Technology.pdf>

[5] John P.Powers, "An introduction to fiber optics Systems," 2nd ed., Tom Casson, USA, 1997

[6] D.Marcuse, "Theory of dielectric optical waveguides," in Theory of Optical Waveguides, New York: Academic Press, 1974

[7] D.Marcuse, D.Gloge, and E.A. Marcatili, "Guiding properties of fibers," in Optical Fiber Telecommunications (S.E. Miller and A.G. Chynoweth, eds.), pp.37-38, New York: Academic Press, 1979

[8] M.Ramsay and G.Hockham, "Propagation in optical fiber waveguides," in Optical Fiber communications (C.Sandbank, ed.), pp.25-29, New York: Wiley, 1980

[9] D.B.Keck, "Optical fiber waveguides," in Fundamentals of Optical Fiber Communications (M.F. Barnoski, ed.), pp.1-107, New York: Academic Press, 1981

[10] Stephen C.Paulov, "Fiber Optic Installation and testing.McGraw-Hill, 2002 sec.9.6

[11] Rajiv Ramaswami and Kumar N.Sivarajan, "Optical Network a Practical Perspective" 2nd ed., pp.49-59, New York: Academic Press, 2001

[12] Govind P.Agrawal, "Optical Communication System," McGraw-Hill, 2001

[13] A.Ghatak, A. Sharma and R.Tewari, "Understanding Fiber Optics on a PC," Viva Books, New Delhi, 1994.

[14]E.A.J.Marcatilli,S.E.Miller:Bell Syst.Tech.J.**48**,2161(1969)

[15] Robert G.Hunsperger Integrated Optics Theory and Technology 4th edition, 1995 pp.83-85

[16] John Gowar, “Optical Communication Systems,’’ prentice hall International Series in Optoelectronics, 2nd ed., pp.89-94, 1993

[17] Govind P.Agrawal, “Nonlinear Fiber Optics,” 2nd. ed., pp.5-7 McGraw-Hill, 2001

[18] Q.Wang,G.Farrell and T.Freir, “Theoretical and Experimental investigation of macrobending in standard single mode fiber,” Appl.Opt.**12**,2(2005)

Appendix A

Miller has shown that light emitted in to a medium from an abruptly terminated waveguide remains collimated to within a waveguide thickness over a length Z_c given by

$$Z_c = \frac{a}{\varphi} = \frac{a^2}{2\lambda_1} \tag{A.1}$$

Where a and f are the near field beam width and far-field angle, and where λ_1 is the wavelength in the medium surrounding the waveguide. The above derivation is based on the fundamental relation from diffraction theory

$$\sin\frac{\varphi}{2} = \frac{\lambda_1}{a} \tag{A.2}$$

Which assumes a sinusoidal distribution of fields in the aperture and requires

$$\alpha \succ \lambda_1 \tag{A.3}$$

The exponential attenuation coefficient is related to the power lost per unit length travelled in the guide by

$$\alpha = -\frac{1}{P(z)}\frac{dP(z)}{d(z)} \tag{A.4}$$

Where P(z) is the power transmitted. Thus, If we define P_l as the power in the tail of the mode beyond X_r (i.e., the power to be lost by radiation within a length Z_c), and P_t as the total power carried by the waveguide, the attenuation coefficient is given by

$$\alpha \cong \frac{1}{p_t}\frac{P_l}{Z_c} \tag{A.5}$$

Where a and f are the near field beam width and far-field angle.

The distance Z_c can be conveniently determined from (1), but Pt must be calculated by integration of the power contained in the optical mode for radii greater than(R+Xc).

If it is assumed that the fields have the form

$$E(x) = \sqrt{C_o}\cos(hx)\ for\ \frac{-a}{2} \le x \le \frac{a}{2}$$

and

$$E(x)=\sqrt{C_o}\cos\left(\frac{ha}{2}\right)\exp\left[-\left(\frac{|x|-\left(\frac{a}{2}\right)}{q}\right)\right] for|x|\geq\frac{a}{2} \tag{A.6}$$

then

$$P_t=\int_{X_{C_c}}^{\infty}E^2(x)dx=C_o\frac{q}{2}\cos^2\left(\frac{ha}{2}\right)\exp\left[\frac{-2}{q}\left(X_c-\frac{a}{2}\right)\right] \tag{A.7}$$

and

$$P_t=\int_{-\infty}^{\infty}E^2(x)dx=C_o\left[\frac{a}{2}+\frac{1}{2h}\sin(ha)+q\cos^2\left(\frac{ha}{2}\right)\right] \tag{A.8}$$

Substituting (7) and (8) in to (4) yields

$$\alpha=\frac{\frac{q}{2}\cos^2\left(\frac{ha}{2}\right)\exp\left(\frac{-2}{q}\frac{\beta_z-\beta_o}{\beta_o}R\right)2\lambda_1\exp\left(\frac{a}{q}\right)}{\left[\frac{a}{2}+\frac{1}{2h}\sin(ha)+q\cos^2\left(\frac{ha}{2}\right)\right]a^2} \tag{A.9}$$

Where $C_1=\dfrac{\frac{q}{2}\cos^2\left(\frac{ha}{2}\right)2\lambda_1\exp\left(\frac{a}{q}\right)}{\left[\frac{a}{2}+\frac{1}{2h}\sin(ha)+q\cos^2\left(\frac{ha}{2}\right)\right]a^2}$

$$C_2=\frac{2}{q}\frac{\beta_z-\beta_o}{\beta_o}$$

While the expression for α in (9) appears quite complex, close scrutiny reveals that it has the relatively simple form,

$$\alpha=C_1\exp(-C_2R)$$

Where C_1 and C_2 are constants that depend on the dimension of the wave guide, the wavelength and the shape of the optical mode.

Appendix B

Optical frequencies and wavelengths

Violet	≈	$7x10^{14}$Hz	0.38-0.48microns
Blue	≈	$6x10^{14}$Hz	0.48-0.52 microns
Green	≈	$5.6x10^{14}$Hz	0.52-0.56 microns
Yellow	≈	$5.1x10^{14}$Hz	0.56-0.62 microns
Orange	≈	$4.8x10^{14}$Hz	0.62-0.64 microns
Red	≈	$4.4x10^{14}$Hz	0.64-0.72 microns